

# Suppression of Microtubule Dynamic Instability and Treadmilling by Deuterium Oxide<sup>†</sup>

Dulal Panda,<sup>‡</sup> Gopal Chakrabarti,<sup>§</sup> Jon Hudson,<sup>§</sup> Karli Pigg,<sup>§</sup> Herbert P. Miller,<sup>‡</sup> Leslie Wilson,<sup>‡</sup> and Richard H. Himes<sup>\*,§</sup>

Department of Molecular Biosciences, University of Kansas, Lawrence, Kansas 66045, and Department of Molecular, Cellular, and Developmental Biology, University of California at Santa Barbara, Santa Barbara, California 93106

Received September 23, 1999; Revised Manuscript Received February 28, 2000

**ABSTRACT:** Deuterium oxide (D<sub>2</sub>O) is known to promote the assembly of tubulin into microtubules *in vitro*, to increase the volume of mitotic spindles and the number and length of spindle microtubules, and to inhibit mitosis. Reasoning that its actions on cellular microtubules could be due to modulation of microtubule dynamics, we examined the effects of replacing H<sub>2</sub>O with D<sub>2</sub>O on microtubule dynamic instability, treadmilling, and steady-state GTPase activity. We found that replacing 50% or more of the H<sub>2</sub>O with D<sub>2</sub>O promoted microtubule polymerization and stabilized microtubules against dilution-induced disassembly. Using steady-state axoneme-seeded microtubules composed of pure tubulin and video microscopy, we found that 84% D<sub>2</sub>O decreased the catastrophe frequency by 89%, the shortening rate by 80%, the growing rate by 50%, and the dynamicity by 93%. Sixty percent D<sub>2</sub>O decreased the treadmilling rate of microtubules composed of tubulin and microtubule-associated proteins by 42%, and 89% D<sub>2</sub>O decreased the steady-state GTP hydrolysis rate by 90%. The mechanism responsible for the ability of D<sub>2</sub>O to stabilize microtubule dynamics may involve enhancement of hydrophobic interactions in the microtubule lattice and/or the substitution of deuterium bonds for hydrogen bonds.

Deuterium oxide (D<sub>2</sub>O)<sup>1</sup> is known to have strong stabilizing effects on protein assemblies. For example, replacement of H<sub>2</sub>O with D<sub>2</sub>O stabilizes the aggregated forms of such diverse oligomeric proteins as phycocyanin (1), lactic dehydrogenase and glutamate dehydrogenase (2),  $\beta$ -lactoglobulin A (3), N<sup>10</sup>-formyltetrahydrofolate synthetase (4), and malate dehydrogenase (5). Assembly processes such as flagellin polymerization (6), the conversion of G-actin to F-actin (7), and the formation of microtubules from tubulin (8–10) are also strongly promoted by D<sub>2</sub>O. The solvent also stabilizes some proteins against inactivation and denaturation (6, 10–16). Several explanations for the effects of D<sub>2</sub>O on protein self-assembly and stability have been proposed, including an increased strength of hydrophobic interactions (15), the greater strength of deuterium bonds compared to hydrogen bonds (3, 6, 11), and changes in the pK<sub>a</sub> values of amino acid side chains (17).

D<sub>2</sub>O appears to affect diverse processes in cells such as microfilament distribution, DNA synthesis, and centrosome function (7, 18–24). A number of studies have demonstrated that D<sub>2</sub>O can block mitosis (reviewed in refs 18 and 19).

This activity is associated with substantial increases in the length and number of mitotic spindle microtubules. Because of the importance of microtubules in such cellular processes as chromosome movement and separation during mitosis and meiosis, vesicle transport, and cellular motility, it would be expected that a change in the number of microtubules, their distribution, or their stability, would have profound effects on cell function.

Microtubules possess two interesting kinetic properties, dynamic instability (25) and treadmilling (26, 27). Dynamic instability refers to the ability of individual microtubules to alternate between states of growth and shortening. This dynamic property aids the microtubule in searching for binding targets such as the kinetochores of chromosomes during mitosis. Treadmilling is the ability of microtubules to grow at their plus ends and shorten at their minus ends. Treadmilling occurs because the critical protein concentrations are different at the two ends. The importance of the dynamic nature of microtubules to mitosis is evident from the fact that both microtubule stabilizing and destabilizing antimitotic drugs suppress dynamic instability *in vitro* (28–31) and in cells (32, 33). Both of the kinetic properties of microtubules, dynamic instability and treadmilling, are altered by a number of microtubule-binding proteins (36–45).

It is possible that the antimitotic action of D<sub>2</sub>O is due to its ability to suppress microtubule dynamics and treadmilling. To test this hypothesis we have examined the effects of D<sub>2</sub>O on the dynamic instability of microtubules *in vitro* by video microscopy and on microtubule treadmilling. We find that that D<sub>2</sub>O strongly suppresses both microtubule kinetic properties.

<sup>†</sup> This research was supported by NIH Grants CA 55141 (R.H.H.) and NS 13560 (L.W.).

<sup>\*</sup> To whom correspondence should be addressed: Telephone (785) 864-3813; Fax (785) 864-5294; E-mail himes@ukans.edu.

<sup>‡</sup> University of California at Santa Barbara.

<sup>§</sup> University of Kansas.

<sup>1</sup> Abbreviations: PEM buffer, 0.1 M 1,4-piperazinediethanesulfonate, 1 mM ethylene glycol bis( $\beta$ -aminoethyl ether)-N,N,N',N'-tetraacetic acid, and 1 mM MgSO<sub>4</sub>, pH 6.9; PMME buffer, 87 mM 1,4-piperazinediethanesulfonate, 36 mM morpholinoethane sulfonate, 1.8 mM MgCl<sub>2</sub>, and 1 mM ethylene glycol bis( $\beta$ -aminoethyl ether)-N,N,N',N'-tetraacetic acid, pH 6.9.

## EXPERIMENTAL PROCEDURES

**Tubulin Purification.** For the treadmilling and dynamic instability experiments, microtubule protein consisting of tubulin containing microtubule-associated proteins (MAPs) was isolated from bovine brain as described previously (45). MAP-free tubulin was purified from this preparation by phosphocellulose chromatography (27). The GTPase experiments were performed with MAP-free tubulin purified by the method of Algaier and Himes (46) from MAP-rich tubulin isolated as described by Tiwari and Suprenant (47).

**Determination of Steady-State Microtubule Polymer Mass.** Tubulin (8  $\mu$ M) was mixed with *Strongylocentrotus purpuratus* flagellar axonemal seeds in 87 mM Pipes, 36 mM Mes, 1.8 mM  $\text{MgCl}_2$ , and 1 mM EGTA, pH 6.9 (PMME buffer), containing 1.5 mM GTP and incubated at 37 °C in the absence and in the presence of different  $\text{D}_2\text{O}$  concentrations for 35 min. The microtubules were pelleted by centrifugation at 48000g for 1 h and the pellets were solubilized in PMME at 0 °C. Protein concentration was determined by the Bradford method (48).

**Analysis of Dynamic Instability.** Tubulin (8  $\mu$ M) was polymerized at the ends of axonemal seeds in PMME buffer in the absence and presence of  $\text{D}_2\text{O}$ . After 35 min of incubation, 3  $\mu$ L of the suspension was prepared for video microscopy. The dynamic instability of individual microtubules was recorded at 37 °C (28). The ends were designated as plus or minus on the basis of the growing rate, the number of microtubules that grew at opposite ends, and their relative lengths (30, 50). Microtubule length changes with time were determined with a computer-based analysis system (a gift from Dr. E. D. Salmon) (28). Data points were collected at 3–5 s intervals. The rates of growing and shortening were determined by least-squares regression analysis of the data points for each growing or shortening phase (28). We considered a microtubule to be in a growing phase if it increased in length by  $>0.2 \mu\text{m}$  at a rate  $>0.15 \mu\text{m}/\text{min}$  and in a shortening phase if it decreased in length by  $>0.2 \mu\text{m}$  at a rate  $>0.3 \mu\text{m}/\text{min}$ . Microtubules showing length changes  $\leq 0.2 \mu\text{m}$  over the duration of six data points were considered to be in an attenuated state. Twenty to thirty microtubules were analyzed for each experimental condition.

**Treadmilling Rates.** The treadmilling rate of MAP-rich microtubules was determined by measuring the incorporation of [ $^3\text{H}$ ]GDP at steady state by a filter assay (49). MAP-rich tubulin (3 mg/mL) was incubated for 40 min at 30 °C in 100 mM Pipes, 1 mM EGTA, and 1 mM  $\text{MgCl}_2$ , pH 6.9 (PEM buffer), containing 0.1 mM GTP and a GTP regenerating system (10 mM acetate kinase and 1 unit/mL acetyl phosphate). Incubations were done in the absence and presence of 60%  $\text{D}_2\text{O}$ . At the end of 40 min, 650  $\mu$ L samples were removed and added to 15  $\mu$ L of [ $^3\text{H}$ ]GTP (15  $\mu\text{Ci}$ ). Samples (40  $\mu$ L) were removed over a 50 min period and added to 4 mL of stabilizing buffer (PEM containing 30% glycerol, 10% DMSO, and 5.6 mM ATP). The stabilized samples were filtered through GF/F glass fiber filters and the filters were washed and counted in a scintillation counter. At the end of 50 min, samples were also removed for mean length and polymer mass determinations.

**GTP Hydrolysis Rates.**  $\text{P}_i$  released as a result of GTP hydrolysis was measured by the malachite green assay (51). Tubulin was polymerized at 37 °C at a concentration of 15

$\mu\text{M}$  in PEM containing 0.5 mM GTP and either 8% DMSO or 89%  $\text{D}_2\text{O}$  or at a concentration of 35  $\mu\text{M}$  in the absence of DMSO or  $\text{D}_2\text{O}$ . At the desired time, 50  $\mu$ L samples were removed and added to 5  $\mu$ L of 70% perchloric acid. After 30 min on ice, the sample was centrifuged for 4 min in a microcentrifuge. The supernatant (40  $\mu$ L) was added to 400  $\mu$ L of a malachite green–ammonium molybdate solution (3 volumes of 0.045% malachite green, 1 volume of 4.2% ammonium molybdate in 4 M HCl, and 0.02 volume of 0.02% Sterox), and after 1 min, 50  $\mu$ L of 34% sodium citrate was added. The absorbance at 650 nm was measured after 30 min. Rates were determined from data between 20 and 45 min.

Samples at 20 and 45 min were also taken to determine microtubule concentrations and polymer mass. The polymerized tubulin concentration was determined by centrifuging a 100  $\mu$ L sample of the assembly reaction after 45 min in a Beckman TL-100 ultracentrifuge at 40000g and 37 °C for 4 min in a TLA-100 rotor. Before centrifugation the sample was first made 0.25% in glutaraldehyde. This was done because we found that microtubules without DMSO or  $\text{D}_2\text{O}$  depolymerized during centrifugation. A control was done to ensure that glutaraldehyde did not cause unpolymerized tubulin to pellet. The concentration of protein in the supernatants was determined and used to calculate the amount of protein in the pellet.

**Microtubule Mean Lengths and Number Concentration.** Electron microscopy was used to determine mean lengths and number concentrations of microtubule populations (44). Samples from the treadmilling and GTP hydrolysis experiments were diluted into PEM-buffered glutaraldehyde, applied to carbon-coated grids, negatively stained with 1% uranyl acetate, and viewed in a Jeol JEM-1200 EX11 at 1000 $\times$  magnification or in a Philips CM 10 electron microscope at 1450 $\times$  magnification. The NIH 1.60 program or Zeiss MOPIII was used to determine the length distribution and mean length (200 microtubules/sample were counted). From this value, the concentration of polymerized tubulin, and a figure of 1690 tubulin dimers/ $\mu\text{m}$  of microtubule, the microtubule number concentration was calculated.

**$\text{D}_2\text{O}$  Solutions.** Buffers containing  $\text{D}_2\text{O}$  were prepared by diluting 10 $\times$  solutions of the components into  $\text{D}_2\text{O}$  or a mixture of  $\text{D}_2\text{O}$  and  $\text{H}_2\text{O}$ . The pH meter readings were taken as the pH or pD of the solutions. To introduce tubulin into the  $\text{D}_2\text{O}$  solutions for the GTPase experiments, tubulin was first assembled into microtubules and pelleted by centrifugation, and the pellets were dissolved in the appropriate solution. For the dynamics and treadmilling experiments a concentrated tubulin solution was diluted into the appropriate  $\text{D}_2\text{O}/\text{H}_2\text{O}$  solution.

## RESULTS

**Effects of  $\text{D}_2\text{O}$  on Axoneme-Seeded Microtubule Polymerization.** We determined the effects of  $\text{D}_2\text{O}$  on the polymerization of tubulin into microtubules by video microscopy. Tubulin at a concentration (0.3 mg/mL) that is below that required for assembly of microtubules at the ends of axoneme seeds in  $\text{H}_2\text{O}$  was incubated with seeds at 37 °C for 30 min in PEM buffer in the absence and presence of 84%  $\text{D}_2\text{O}$ . The number of microtubules nucleated at the ends of 200 seeds was determined. As expected in the  $\text{H}_2\text{O}$  control, no

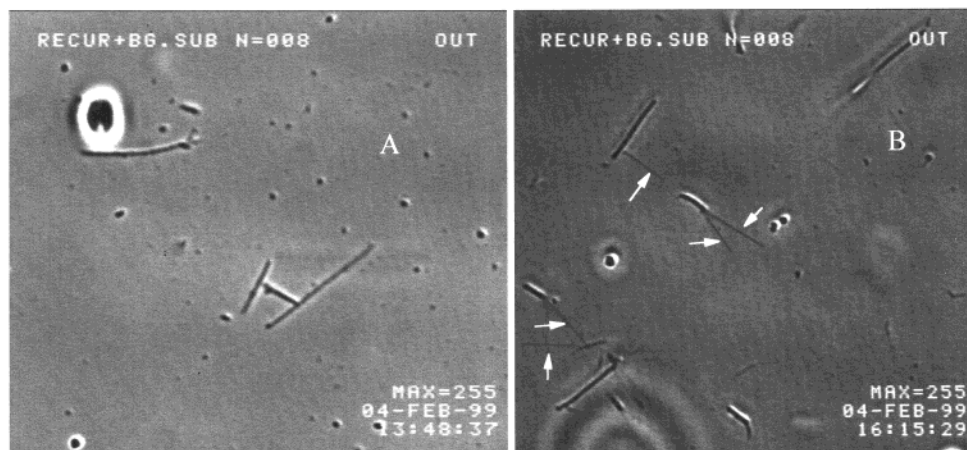


FIGURE 1: Effect of D<sub>2</sub>O on the stability of microtubules against dilution-induced disassembly. Tubulin (30  $\mu$ M) was polymerized at the ends of axonemal seeds for 30 min in PEM. Preformed microtubules were diluted (1:30) in tubulin-free PEM in the absence (A) or presence (B) of 87% D<sub>2</sub>O. The arrows point to microtubules.

microtubules formed at the ends of the seeds (data not shown). However, 84% D<sub>2</sub>O strongly promoted polymerization. Greater than 90% of the axoneme seeds contained one or more microtubules. Similar effects occurred at 64% D<sub>2</sub>O (data not shown). These results demonstrate that D<sub>2</sub>O strongly promotes microtubule assembly.

**Stabilization of Microtubules against Dilution-Induced Disassembly.** We wanted to determine whether D<sub>2</sub>O could stabilize microtubules. Thus, we determined the effects of D<sub>2</sub>O on dilution-induced microtubule disassembly in two ways. In the first, tubulin (3.0 mg/mL) was polymerized in PEM buffer at the ends of axoneme seeds. We then diluted the microtubules 30-fold to 0.1 mg/mL into PEM buffer either in H<sub>2</sub>O or in 87% D<sub>2</sub>O to obtain a qualitative determination of whether D<sub>2</sub>O could stabilize microtubules. The seeds contained between two and four microtubules prior to dilution as revealed by video microscopy. Thirty minutes after dilution in H<sub>2</sub>O, the seeds contained no microtubules (Figure 1A). However, >95% of the axonemes retained one or two microtubules when diluted into 87% D<sub>2</sub>O (Figure 1B). While the microtubules were fewer in number and shorter than those in the undiluted sample, indicating that some disassembly had occurred, the results show clearly that D<sub>2</sub>O strongly stabilized microtubules.

In the second approach, we assembled microtubules rich in microtubule-associated proteins in the absence of seeds to polymer mass steady state and pulsed the suspension with a trace of [<sup>3</sup>H]GTP for 45 min to label the microtubule plus ends with [<sup>3</sup>H]GDP in the e-site of  $\beta$ -tubulin (49). One portion of the microtubule suspension was diluted into water-based buffer and the second was diluted into buffer containing 89% D<sub>2</sub>O. The microtubules were collected at various times after dilution and the amount of radiolabeled GDP-tubulin was determined by a filter assay (49). The D<sub>2</sub>O reduced the rate of dilution-induced dissociation of tubulin from the microtubule ends approximately 4-fold, from 17.5 to 4.5 s<sup>-1</sup>.

**Effects of D<sub>2</sub>O on Dynamic Instability.** To analyze the effects of D<sub>2</sub>O on dynamic instability with axonemal-seeded microtubules, it was first necessary to determine the effects of D<sub>2</sub>O on the mass of microtubule growth at the ends of the seeds. Tubulin (8  $\mu$ M) was polymerized at the ends of the seeds in the absence and presence of different concentra-

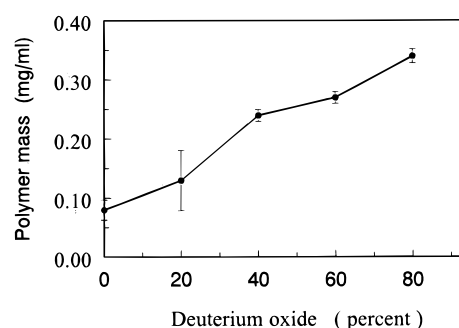


FIGURE 2: Effect of D<sub>2</sub>O on microtubule polymer mass. Tubulin (8  $\mu$ M) was polymerized in the absence or presence of different concentrations of D<sub>2</sub>O as described under Experimental Procedures.

tions of D<sub>2</sub>O and the microtubule mass was determined by centrifugation 35 min after initiation of polymerization. As shown in Figure 2, D<sub>2</sub>O strongly increased the microtubule mass in a concentration-dependent manner. For example, 20% D<sub>2</sub>O increased the mass 1.7-fold and 80% D<sub>2</sub>O increased the mass 4.4-fold.

We then determined the effects of D<sub>2</sub>O on the dynamic instability behavior of the microtubules *in vitro*. At the time analysis was begun (35 min), control microtubules had reached a minimum of 80% of the steady-state polymer level. In the H<sub>2</sub>O control, the microtubules grew only at the plus ends, and in the presence of high concentrations of D<sub>2</sub>O, they also grew predominantly at the plus ends. Several life history traces of length changes of individual microtubules in the absence (Figure 3A) or presence (Figure 3B) of D<sub>2</sub>O are shown. Control microtubules spent most of the time in the growing and shortening phases and only a small fraction of time in an attenuated state (pause), with no detectable growing or shortening. It is clear that D<sub>2</sub>O strongly suppressed the dynamic instability behavior of the microtubules, as they spent most of the time in an attenuated state.

The quantitative effects of D<sub>2</sub>O on all of the measured dynamic instability parameters are shown in Table 1. The effects of D<sub>2</sub>O on the growing and shortening rates are shown in Figure 4. D<sub>2</sub>O strongly suppressed the shortening rate in a concentration dependent manner (Table 1, Figure 4). For example, 84% D<sub>2</sub>O reduced the shortening rate by 79% from 30  $\pm$  3.9 to 6.2  $\pm$  2.8  $\mu$ m/min. On the other hand, D<sub>2</sub>O did not affect the growing rate until the D<sub>2</sub>O concentration in



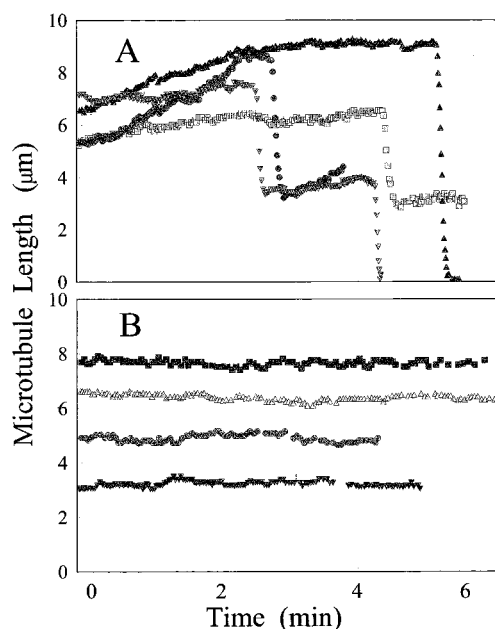


FIGURE 3: Growing and shortening length changes of microtubules at plus ends in the absence (A) or presence (B) of 84% D<sub>2</sub>O. Length changes of individual microtubules with time were determined as described under Experimental Procedures.

Table 1: Effects of D<sub>2</sub>O on Dynamic Instability Parameters of Individual Microtubules<sup>a</sup>

parameter	D <sub>2</sub> O concentration			
	0%	20%	62%	84%
Rate (μm/min)				
growing	0.65 ± 0.10	0.72 ± 0.13	0.71 ± 0.07	0.32 ± 0.10
shortening	30.0 ± 3.9	26.2 ± 4.4	12.8 ± 2.5	6.2 ± 2.8
Average length				
Excursion (μm/event)				
growing	1.8 ± 0.56	1.2 ± 0.25	1.71 ± 0.2	0.47 ± 0.08
shortening	3.4 ± 0.45	3.9 ± 0.53	3.6 ± 0.7	2.0 ± 0.88
Transition				
Frequency (min <sup>-1</sup> )				
catastrophe	0.28 ± 0.07	0.3 ± 0.07	0.14 ± 0.04	0.032 ± 0.01
rescue	3.8 ± 0.45	2.4 ± 0.8	3.0 ± 0.83	2.4 ± 1.1
Time Spent in Phase (%)				
growing	80	67.3	73	17.7
shortening	3.2	6.4	4.1	1.1
attenuation	16.7	26.3	22.9	81.2
Dynamicity (μm/min)				
	1.43	1.5	0.93	0.1

<sup>a</sup> ± values refer to SD except for rates of growing and shortening, which are SEM.

the solution was higher than 62% (Figure 4). At 84% D<sub>2</sub>O, the growing rate was reduced by 50% from  $0.65 \pm 0.1$  to  $0.32 \pm 0.1$ . D<sub>2</sub>O also significantly increased the time microtubules spent in the attenuated state. Interestingly, 62% D<sub>2</sub>O increased the polymer mass by 3.5-fold and therefore reduced the soluble tubulin-GTP concentration from 7.2 to 5.2 μM. Despite the reduction in the concentration of soluble tubulin, the growth rate did not decrease (Figures 2 and 4). Thus, D<sub>2</sub>O must reduce the rate of tubulin dissociation from microtubules or increase the association rate constant (see Discussion).

The switching frequency is a reflection of the mechanism of gain and loss of the stabilizing cap at microtubule ends. D<sub>2</sub>O strongly suppressed the catastrophe frequency (the

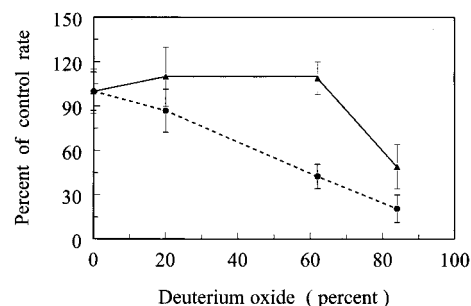


FIGURE 4: Effects of D<sub>2</sub>O on the growing (▲) and shortening (●) rates. The growing and shortening rates were determined as described under Experimental Procedures. The error bars represent the SEM.

transition from growing or attenuation to shortening) in a concentration-dependent fashion. However, it did not appreciably affect the rescue frequency (Table 1). In the presence of 84% D<sub>2</sub>O the catastrophe frequency was reduced by 90%, from  $0.28 \pm 0.07$  to  $0.032 \pm 0.01$ , suggesting that D<sub>2</sub>O might affect the capping mechanism.

Dynamicity is the measure of all detectable dimer exchange at the microtubule ends (the total detectable tubulin dimer addition and loss at a microtubule end including the time the microtubules spend in the attenuated state) (28, 45). It reflects the extent to which an agent kinetically stabilizes a microtubule. As shown in Table 1, D<sub>2</sub>O strongly suppressed the dynamicity; 84% D<sub>2</sub>O reduced the dynamicity by 93%, and thus, strongly stabilizes microtubules.

The dynamic instability experiments were done in buffers having identical pH meter readings. However, because of the difference in the glass electrode response to H<sup>+</sup> and D<sup>+</sup>, a correction must be made for solutions containing D<sub>2</sub>O to obtain the pD value (52). While the pH meter reading was 6.9, the true pD value for an 85% D<sub>2</sub>O solution is about 7.2. To ensure that this difference was not responsible for the large difference in dynamic instability, we determined the effects of elevated pH on the dynamics of individual microtubules. We found that the overall dynamicity was 1.38 μm/min at pH 7.2, compared to 1.43 μm/min at pH 6.9 (data not shown). Thus, the suppressed microtubule dynamics observed in the presence of D<sub>2</sub>O were not due to differences in the pH and pD values.

**Effects of D<sub>2</sub>O on the Treadmilling Rate of MAP-Rich Microtubules.** Treadmilling is mechanistically distinct from dynamic instability. It occurs because the critical subunit concentrations at the opposite microtubule ends are different (27). The effect of D<sub>2</sub>O on treadmilling was determined with MAP-rich microtubules and [<sup>3</sup>H]GTP exchange methodology (49). Both dynamic instability and treadmilling give rise to incorporation of [<sup>3</sup>H]GDP into the microtubules. However, MAP-rich microtubules show little dynamic instability behavior (44, 45) and the linear incorporation of [<sup>3</sup>H]GDP that occurs after the initial burst of incorporation due to dynamic instability at the extreme ends of the microtubules is due primarily to treadmilling (see ref 44). Microtubule protein (tubulin plus MAPs) was polymerized to polymer mass steady state, at which time the microtubules were pulsed with [<sup>3</sup>H]GTP. The kinetics of [<sup>3</sup>H]GDP-tubulin incorporation into the microtubules were determined (Figure 5) and the treadmilling rate was calculated from the linear portion of the data. The treadmilling rate was 0.48 μm/h in H<sub>2</sub>O,

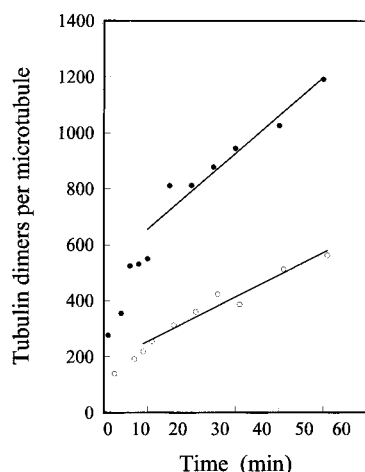


FIGURE 5: Suppression of the treadmilling rate by 60% D<sub>2</sub>O. MAP-rich tubulin (3 mg/mL) was polymerized to steady state in PEM buffer. Microtubules were pulsed with [<sup>3</sup>H]GTP and the kinetics of [<sup>3</sup>H]GDP incorporation into the microtubules were determined as described under Experimental Procedures. The mean length of the microtubules was 13.6  $\mu$ m in the absence of D<sub>2</sub>O (●) and 8.8  $\mu$ m in its presence (○), indicative of a greater degree of nucleation in D<sub>2</sub>O.

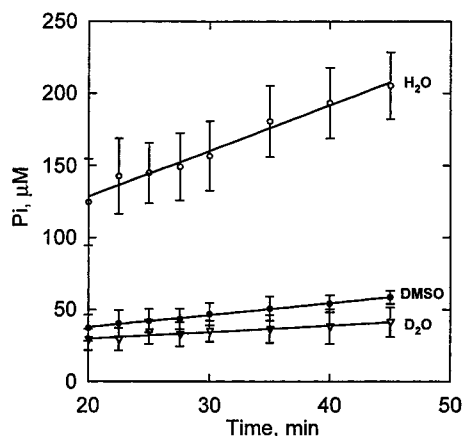


FIGURE 6: Rates of P<sub>i</sub> formation. Assembly reactions were performed and P<sub>i</sub> measured after steady state was reached as described under Experimental Procedures. The *n* values were 6 for H<sub>2</sub>O, 4 for DMSO, and 8 for D<sub>2</sub>O.

consistent with previous reports (44). D<sub>2</sub>O (60%) reduced the treadmilling rate 42% to 0.28  $\mu$ m/h.

**Effect of D<sub>2</sub>O on the Steady-State GTPase Activity.** Because of the dynamic nature of steady-state microtubules, they constantly hydrolyze GTP in association with tubulin exchange. The level of GTPase activity is a measure of the dynamic nature of the microtubules; stable microtubules would be expected to have low rates of GTP hydrolysis. We measured the GTPase activity of microtubules assembled in the absence of seeds in H<sub>2</sub>O, in D<sub>2</sub>O, and, for comparison, in the presence of 8% DMSO, a known microtubule stabilizing agent (46). The kinetics of P<sub>i</sub> release in the presence of H<sub>2</sub>O, D<sub>2</sub>O, and DMSO are presented in Figure 6. The mean rate of P<sub>i</sub> formation was  $3.31 \pm 0.72 \mu\text{M}/\text{min}$  in H<sub>2</sub>O,  $0.48 \pm 0.21 \mu\text{M}/\text{min}$  in D<sub>2</sub>O, and  $0.84 \pm 0.28 \mu\text{M}$  in 8% DMSO. The rate of GTP hydrolysis is proportional to the number concentration of microtubules, but we found that this value was almost the same for the three assembly conditions. In Table 2 the rates of GTP hydrolysis per microtubule are presented for one experiment. The rate per

Table 2: GTPase Activity of Microtubules at Steady State<sup>a</sup>

solvent	MT mean length ( $\mu$ m)	concentration of MTs (nM)	P <sub>i</sub> formation ( $\mu$ M/min)	P <sub>i</sub> formation (P <sub>i</sub> min <sup>-1</sup> MT <sup>-1</sup> )
H <sub>2</sub> O	23.1 $\pm$ 13.5	0.37	3.32	8973
D <sub>2</sub> O	16.7 $\pm$ 7.2	0.41	0.33	805
DMSO	11.5 $\pm$ 6.3	0.51	0.86	1686

<sup>a</sup> Assembly reactions and rate determinations were carried out as described under Experimental Procedures. The concentration of assembled tubulin was 14.3  $\mu$ M in H<sub>2</sub>O, 11.6  $\mu$ M in D<sub>2</sub>O, and 10  $\mu$ M in DMSO. The length measurements were taken at the 20 min time point after assembly was initiated. Length measurements also done at the 45 min time point gave the following mean lengths: H<sub>2</sub>O, 22.1  $\pm$  13.9  $\mu$ m; D<sub>2</sub>O, 19.5  $\pm$  10.8  $\mu$ m; and DMSO, 11.9  $\pm$  6.3  $\mu$ m.

microtubule in D<sub>2</sub>O (805 P<sub>i</sub> min<sup>-1</sup> MT<sup>-1</sup>) was about 10% of that in H<sub>2</sub>O (8973 P<sub>i</sub> min<sup>-1</sup> MT<sup>-1</sup>). The rates of 1686 and 805 P<sub>i</sub> min<sup>-1</sup> MT<sup>-1</sup> in 8% DMSO and D<sub>2</sub>O, respectively, compare to a rate of 1808 P<sub>i</sub> min<sup>-1</sup> MT<sup>-1</sup> for porcine brain microtubules (53) and 1500 P<sub>i</sub> min<sup>-1</sup> MT<sup>-1</sup> for yeast microtubules (54), both in 1 M glycerol. Thus similar to the DMSO, D<sub>2</sub>O strongly suppresses GTP hydrolysis at microtubule ends, consistent with the idea that it strongly stabilizes microtubules.

## DISCUSSION

It is clear from the data presented in this work that D<sub>2</sub>O has a very strong stabilizing effect on microtubules. D<sub>2</sub>O strongly promoted microtubule assembly and stabilized microtubules against dilution-induced disassembly. It also strongly suppressed the dynamic instability behavior of axoneme-seeded MAP-free microtubules by reducing the catastrophe frequency and the shortening rate. Finally, it suppressed the treadmilling rate of MAP-rich microtubules, and it inhibited the rate of GTP hydrolysis of microtubules at steady state.

**Effect of D<sub>2</sub>O on the Catastrophe Frequency.** D<sub>2</sub>O strikingly reduced the catastrophe frequency. For example, 84% D<sub>2</sub>O reduced the catastrophe frequency by 89%. A microtubule will continue to grow as long as it maintains a stabilizing GTP or GDP-P<sub>i</sub> cap at its end. Loss of the cap induces a catastrophe and the microtubule rapidly loses subunits. The catastrophe frequency, therefore, is a reflection of the loss of the stabilizing cap. It is reasonable to think that the decrease in the catastrophe frequency in D<sub>2</sub>O is a reflection of the suppression of microtubule dynamics, caused either by a greater stability of the microtubule lattice or by a reduction in the dissociation of tubulin-GTP or tubulin-GDP-P<sub>i</sub> from the microtubule end. Alternatively, D<sub>2</sub>O may suppress the catastrophe frequency by having a direct effect on the hydrolysis rate. However, we feel this is a less likely possibility (see below).

**Effect of D<sub>2</sub>O on Shortening and Growing Rates.** D<sub>2</sub>O reduced the shortening rate dramatically (Figure 4). These results support the idea that D<sub>2</sub>O stabilizes dimer-dimer bonds in the lattice. Although it is not known how D<sub>2</sub>O might stabilize microtubules, one reasonable possibility consistent with other data (15) is that it increases the strength of hydrophobic interactions between tubulin dimers in the lattice. It is commonly accepted that hydrophobic interactions are important in dimer-dimer interactions in the microtubule lattice (54). This concept receives further support from the finding that mutations at three conserved leucine residues

in  $\beta$ -tubulin, L215, L217, and L228, destabilize microtubules (56). L215 and L217 are located in a loop between helices 6 and 7 in  $\beta$ -tubulin, and L228 is located within helix 7 (57). The electron crystal structure of tubulin and a 20 Å map of the microtubule indicate that this region is involved in both lateral and longitudinal contacts in the microtubule (57).

The effect of D<sub>2</sub>O on the growing rate was complex (Figure 4). At low and intermediate concentrations (20% and 62%), D<sub>2</sub>O did not alter the growing rate; however, it did reduce the growing rate at a high (84%) concentration. The growing rate at a microtubule end depends on the association rate constant, the dissociation rate constant, and the concentration of free tubulin, according to the relationship  $r_g = k_+C - k_-$ , where  $r_g$  is the growing rate,  $k_+$  is the association rate constant,  $k_-$  is the dissociation rate constant, and  $C$  is the soluble tubulin dimer concentration. The microtubule polymer mass increased in D<sub>2</sub>O, and therefore, the soluble tubulin dimer concentration decreased. For example, 60% D<sub>2</sub>O increased the polymer mass by 350% compared to that in H<sub>2</sub>O (Figure 2). In the control microtubule suspension the soluble tubulin concentration was 7.2  $\mu$ M, and in the presence of 62% D<sub>2</sub>O, the soluble tubulin concentration was 5.2  $\mu$ M. Thus, a 25% decrease in the tubulin concentration did not result in a noticeable change in the growth rate. This result could be explained by a decrease in the dissociation rate constant, an increase in the association rate constant, or a combination of both. Evidence obtained by dilution-induced disassembly (see Results) indicates that D<sub>2</sub>O strongly reduces the dissociation rate constant. At a high concentration (84%), D<sub>2</sub>O did reduce the growing rate, which probably is due to reduction of the soluble tubulin concentration.

**Effect on Steady-State GTP Hydrolysis.** It is possible that D<sub>2</sub>O could directly decrease the rate of hydrolysis. As a general rule, the rate of hydrolysis of a reaction where the transfer of an exchangeable hydrogen is the rate-limiting step would be decreased by D<sub>2</sub>O (58). Thus, the decrease in microtubule dynamics by D<sub>2</sub>O could be due to a decrease in the GTPase activity of microtubules in the presence of D<sub>2</sub>O. However, previously we showed that the drug-stimulated GTPase activity of tubulin is increased by D<sub>2</sub>O, i.e., there is an inverse solvent isotope effect (59). Assuming the chemical mechanism of hydrolysis of GTP during addition of tubulin to a microtubule is identical to the mechanism of the drug-induced GTPase activity, we would have expected an increase in steady-state GTP hydrolysis in the absence of other considerations. We therefore propose that the decreased dynamics of the microtubules explains the large decrease in the steady-state rate of GTP hydrolysis, although it is certainly possible that the solvent isotope effect on the steady-state hydrolysis of GTP may differ from the effect on the drug-induced hydrolysis by unpolymerized tubulin.

**D<sub>2</sub>O as an Antimitotic and Antiproliferative Agent.** The antimitotic effects of D<sub>2</sub>O require high D<sub>2</sub>O concentrations. Its effects on mitosis also vary among cell types. For example, 50% D<sub>2</sub>O causes a substantial increase in spindle size in marine oocytes (18, 19) and grasshopper spermatocytes (60) but not in mammalian cells (23, 61, 62). When cells are exposed to ~50% or less D<sub>2</sub>O, mitosis still proceeds but usually at a slower rate than normal (60, 61). Concentrations of 75–80% inhibit cell proliferation during late G2 and early mitosis (21, 23, 24, 61). Our data suggest that the mitotic block induced by high concentrations of D<sub>2</sub>O may

be due to suppression of both the catastrophe frequency and the shortening rate of mitotic microtubules. However, D<sub>2</sub>O is also known to exert antiproliferative activity during interphase. The fact that D<sub>2</sub>O strongly suppresses the dynamic instability and treadmilling of microtubules suggests D<sub>2</sub>O might inhibit cell proliferation during interphase by stabilizing the interphase microtubule cytoskeleton. Disassembly of the interphase microtubule network is a prerequisite for the formation of mitotic spindles and D<sub>2</sub>O might prevent the disassembly.

## REFERENCES

- Berns, S. D., Lee, J. J., and Scott, E. (1968) in *Molecular Association in Biological and Related Systems* (Gould, R. F., Ed.) Advances in Chemistry Series, pp 21–30, American Chemical Society, Washington, DC.
- Henderson, R. F., Henderson, T. R., and Woodfin, B. H. (1970) *J. Biol. Chem.* 245, 3733–3737.
- Baghurst, P. A., Nichol, L. W., and Sawyer, W. H. (1972) *J. Biol. Chem.* 247, 3198–3204.
- Harmony, J. A. K., Himes, R. H., and Schowen, R. L. (1975) *Biochemistry* 14, 5379–5386.
- Bonneté, F., Madern, D., and Zaccari, G. (1994) *J. Mol. Biol.* 244, 436–477.
- Uratani, Y. (1974) *J. Biochem. (Tokyo)* 75, 1143–1151.
- Omori, H., Kuroda, M., Naora, H., Takeda, H., Nio, Y., Otani, H., and Tamura, K. (1997) *Eur. J. Cell Biol.* 74, 273–280.
- Houston, L. L., Odell, J., Lee, Y. C., and Himes, R. H. (1974) *J. Mol. Biol.* 87, 141–146.
- Ito, T. J., and Sato, H. (1984) *Biochim. Biophys. Acta* 800, 21–27.
- Chakrabarti, G., Kim, S., Gupta, M. L., Jr., Barton, J. S., and Himes, R. H. (1999) *Biochemistry* 38, 3067–3072.
- Maybury, R. H., and Katz, J. J. (1956) *Nature* 177, 629–630.
- Hermans, J., Jr., and Scheraga, H. A. (1959) *Biochim. Biophys. Acta* 36, 534–535.
- Dong, A., Kendrick, B., Kreilgård, L., Matsuura, J., Manning, M. C., and Carpenter, J. F. (1997) *Arch. Biochem. Biophys.* 347, 213–220.
- Verheul, M., Roefs, S. P. F. M., and de Kruif, K. G. (1998) *FEBS Lett.* 421, 273–276.
- Kresheck, G. C., Schneider, H., and Scheraga, H. A. (1965) *J. Phys. Chem.* 69, 3132–3144.
- Lemm, U., and Wenzel, M. (1981) *Eur. J. Biochem.* 116, 441–445.
- Itzhaki, L. S., and Evans, P. A. (1996) *Protein Sci.* 5, 140–146.
- Sato, H., Kato, T., Takahashi, T. C., and Ito, T. (1982) in *Biological Functions of Microtubules and Related Structures* (Sakai, H. Mohri, H., and Borisy, G. G., Eds.) pp 211–226, Academic Press, New York.
- Krendel, M., and Inoué, S. (1995) *Biol. Bull.* 189, 204–205.
- Zimmermann, A., Keller, H.-U., and Cottier, H. (1988) *Eur. J. Cell Biol.* 47, 320–326.
- Schroeter, D., Lamprecht, J., Eckhardt, R., Futterman, G., and Paweletz, N. (1992) *Eur. J. Cell Biol.* 58, 365–370.
- Lamprecht, J., Schroeter, D., and Paweletz, N. (1991) *J. Cell Sci.* 98, 463–473.
- Lamprecht, J., Schroeter, D., and Paweletz, N. (1989) *Eur. J. Cell Biol.* 50, 360–369.
- Lamprecht, J., Schroeter, D., and Paweletz, N. (1990) *Eur. J. Cell Biol.* 51, 303–312.
- Mitchison, T., and Kirschner, M. (1984) *Nature* 312, 237–242.
- Margolis, R. L., and Wilson, L. (1978) *Cell* 13, 1–8.
- Panda, D., Miller, H. P., and Wilson, L. (1999) *Proc. Natl. Acad. Sci. U.S.A.* 96, 12459–12464.
- Panda, D., Daijo, J. E., Jordan, M. A., and Wilson, L. (1995) *Biochemistry* 34, 9921–9929.
- Derry, W. B., Wilson, L., and Jordan, M. A. (1995) *Biochemistry* 34, 2203–2211.

30. Panda, D., Jordan, M. A., Chu, K. C., and Wilson, L. (1996) *J. Biol. Chem.* 271, 29807–29812.
31. Panda, D., Himes, R. H., Moore, R. E., Wilson, L., and Jordan, M. A. (1997) *Biochemistry* 36, 12948–12953.
32. Dhamodharan, R., Jordan, M. A., Thrower, D., Wilson, L., and Wadsworth, P. (1995) *Mol. Biol. Cell* 6, 1215–1229.
33. Yvon, A.-M. C., Wadsworth, P., and Jordan, M. A. (1999) *Mol. Biol. Cell* 10, 947–959.
34. Pryer, N. K., Walker, R. A., Skeen, V. P., Bourns, B. D., Soboeiro, M. F., and Salmon, E. D. (1992) *J. Cell Sci.* 103, 965–976.
35. Drechsel, D. N., Hyman, A. A., Cobb, M. H., and Kirschner, M. W. (1992) *Mol. Biol. Cell* 3, 1141–1154.
36. Kowalski, R. J., and Williams, R. C., Jr. (1993) *J. Biol. Chem.* 268, 9847–9855.
37. Panda, D., Goode, B. L., Feinstein, S. C., and Wilson, L. (1995) *Biochemistry* 34, 11117–11127.
38. Dhamodharan, R., and Wadsworth, P. (1995) *J. Cell Sci.* 108, 1679–1689.
39. Belmont, L. D., and Mitchison, T. J. (1996) *Cell* 84, 623–631.
40. Walczak, C. E., Mitchison, T. J., and Desai, A. (1996) *Cell* 84, 37–47.
41. Gamblin, T. C., Nachmanoff, K., Halpain, S., and Williams, R. C., Jr. (1996) *Biochemistry* 35, 12576–12586.
42. Vandecandelaere, A., Pedrotti, B., Utton, M. A., Calvert, R. A., and Bayley, P. M. (1996) *Cell Motil. Cytoskel.* 35, 134–146.
43. Hamill, D. R., Howell, B., Cassimeris, L., and Suprenant, K. A. (1998) *J. Biol. Chem.* 273, 9285–9291.
44. Farrell, K. W., Jordan, M. A., Miller, H. P., and Wilson, L. (1987) *J. Cell Biol.* 104, 1035–1046.
45. Toso, R. J., Jordan, M. A., Farrell, K. W., Matsumoto, B., and Wilson, L. (1993) *Biochemistry* 32, 1285–1293.
46. Algaier, J., and Himes, R. H. (1988) *Biochim. Biophys. Acta* 954, 235–243.
47. Tiwari, S. C., and Suprenant, K. A. (1993) *Anal. Biochem.* 215, 96–103.
48. Bradford, M. M. (1976) *Anal. Biochem.* 72, 248–254.
49. Wilson, L., Snyder, K. B., Thompson, W. C., and Margolis, R. L. (1982) *Meth. Cell Biol.* 24, 159–169.
50. Walker, R. A., O'Brien, E. T., Pryer, N. K., Soboeiro, M. F., Voter, W. A., Erickson, H. P., and Salmon, E. D. (1988) *J. Cell Biol.* 107, 1437–1448.
51. Lanzetta, P. A., Alvarez, L. J., Reinach, P. S., and Candia, O. A. (1979) *Anal. Biochem.* 100, 95–97.
52. Schowen, K. B., and Schowen, R. L. (1982) *Methods Enzymol.* 87, 551–606.
53. Vandecandelaere, A., Brune, M., Webb, M. R., Martin, S. R., and Bayley, P. M. (1999) *Biochemistry* 38, 8179–8188.
54. Dougherty, C. A., Himes, R. H., Wilson, L., and Farrell, K. W. (1998) *Biochemistry* 37, 10861–10865.
55. Correia, J. J., and Williams, R. C., Jr. (1983) *Annu. Rev. Biophys. Bioeng.* 12, 211–235.
56. Gonzalez-Garay, M. L., Chang, L., Blade, K., Menick, D. R., and Cabral, F. (1999) *J. Biol. Chem.* 274, 23875–23882.
57. Nogales, E., Whittaker, M., Milligan, R. A., and Downing, D. H. (1999) *Cell* 96, 79–88.
58. Schowen, K. B. J. (1978) in *Transition States of Biochemical Processes* (Gandour, R. D., and Schowen, R. L., Eds.) pp 225–283, Plenum Press, New York.
59. Mejillano, M. R., Shivanna, B. D., and Himes, R. H. (1996) *Arch. Biochem. Biophys.* 336, 130–138.
60. Sumitro, S. B., Izutsu, S., and Sato, H. (1989) *Cell Struct. Funct.* 14, 345–352.
61. Leonard, P. J., and Mullins, J. M. (1987) *Exp. Cell Res.* 172, 204–211.
62. McIntosh, R. (1979) in *Microtubules* (Roberts, K., and Hyams, J. S., Eds.) pp 381–441, Academic Press, London.

BI992217F